# 1

# Fundamentals of Polymer

## 1.1 What Is Polymer?

The "poly" in polymer means "many," and polymers are also known as "macromolecules." As the name suggests, they are substances with high molecular weights. Due to this high molecular weight, polymers exhibit quite unique properties which are completely different from other materials, such as inorganic materials, metallic materials, and organic low-molecular-weight materials. Thermal expansion, which will be explained in Chapter 2 and beyond, is one of these properties. Some readers may not be familiar with polymers, so we would like to briefly review the fundamentals of polymers in this chapter. However, there are some parts that are explained from our own perspective, which may cause some readers to feel confused. Thus, we ask you for your understanding.

This chapter is intended for readers who are not very familiar with polymers. If you have a good knowledge of polymers, you can skip this chapter and start from the next chapter, Chapter 2.

### 1.1.1 What Molecular Weight Should a Substance Be Defined as "Polymer"?

What molecular weight should a substance be defined as a polymer? To tell the truth, there is no clear definition. Here, we will introduce one of the generally accepted definitions. As the molecular weight increases, the size and length of the molecules also increase. When they reach a certain length, entanglement between molecules begins. The molecular weight at which this entanglement begins is called a molecular weight between entanglements, $M_e$.

So how can $M_e$ be obtained? In principle, there are two methods to obtain $M_e$. One is to track the time, frequency, or temperature changes in the viscoelastic functions of a concentrated polymer solution or a polymer melt. Figure 1.1 shows the time dependence of storage modulus for typical amorphous polymer. Depending upon the state of the polymer, the viscoelastic function (in this case, storage modulus) can be divided into four regions: glassy, transition, rubbery plateau, and flow regions. In the rubbery-plateau region, the viscoelastic function loses its time (temperature)

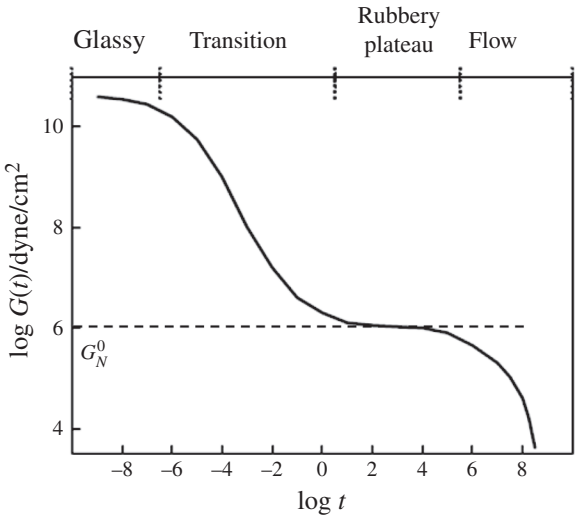


**Figure 1.1** Typical viscoelastic function behavior on time for an amorphous polymer.

dependency and becomes flat. The reason for the loss of time dependency is interpreted to be that some kind of network due to the molecular entanglements is formed, which leads to elimination of relaxation and thus causes the system to become elastic.

The height of this rubbery-plateau region is called the pseudo-equilibrium modulus $G_N^0$, and has the following relationship with the $M_e$.

$$G_N^0 = \frac{\rho RT}{M_e} \tag{1.1}$$

or

$$M_e = \frac{\rho RT}{G_N^0} \tag{1.2}$$

where $\rho$, $R$, and $T$ are density, gas constant, and absolute temperature, respectively.

As seen from those formulas, $M_e$ and $G_N^0$ are inversely proportional, and the molecule with a lower $M_e$, in other words, more entanglements is supposed to have higher $G_N^0$. By determining $G_N^0$ from viscoelasticity measurements, we can obtain $M_e$ by using the formula (1.1) or (1.2).

We will now introduce another method. This is a method for determining $M_e$ from a plot of viscosity and molecular weight. Please take a look at Figure 1.2 [1]. This is a plot of the relationship between zero-shear melt viscosity measured at 217 °C and weight-average molecular weight for polystyrene (PS). When plotted on a logarithmic scale, the relationship between the two becomes linear. Hence, a viscosity $\eta$ and molecular weight $M$ have a power relationship as shown in the formula (1.3).

$$\eta \propto M^{\alpha} \tag{1.3}$$

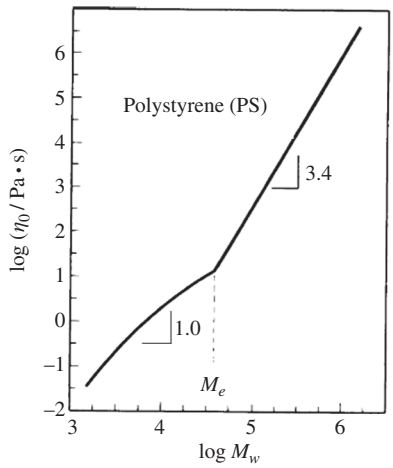


**Figure 1.2** Relationship between weight-average molecular weight and zero-shear melt viscosity at 217 °C for PS [1].

However, we can see that the slope of the line changes at a certain molecular weight. This molecular weight is defined as $M_e$. When the length of the molecules exceeds the one corresponding to a certain limit $M_e$, the molecules begin to entangle. When $M < M_e$, $\alpha = 1.0 \sim 2.0$, while when $M > M_e$, $\alpha = 3.0 \sim 4.0$. In other words, the molecular entanglements increase the sensitivity of viscosity to molecular weight.

This method is time-consuming because it requires measuring the viscosity of polymers with multiple molecular weights, but unlike the method by viscoelastic measurement, it has the advantage of being able to directly obtain $M_e$ without using a conversion formula such as the formulas (1.1) and/or (1.2).

Now let us investigate the relationship between $M_e$ and the molecular structure of a polymer. In fact, $M_e$ varies greatly depending on the molecular structure of a polymer. Table 1.1 summarizes the $M_e$ and $C_\infty$ of various polymers, where $C_\infty$ is a parameter that indicates the flexibility of the molecular chain, called the characteristic ratio, and is defined by the formula (1.4).

$$C_\infty = \lim_{n\to\infty}\left\{\frac{\langle R_0{}^2\rangle}{n\langle l^2\rangle}\right\} \tag{1.4}$$

where $\langle R_0{}^2\rangle$ is the root mean square of the end-to-end distance of a molecular chain, $n$ is the bendable bond unit, and $\langle l^2\rangle$ is the root mean square length of the bendable bond unit. Here, the bendable bond unit refers to the C—C bond in the main chain. The bending of the main chain containing bulky functional groups, double bonds, and aromatic rings are restricted, thus its $\langle l^2\rangle$ becomes small. In other words, its $C_\infty$ becomes higher.

Furthermore, the relationship between $M_e$ and $C_\infty$ is expressed by the formula (1.5) [2]. Here, $M_v$ is the molecular weight of the repeating unit.

$$M_e = 3M_v C_\infty{}^2 \tag{1.5}$$

**Table 1.1** $M_e$ and characteristic ratio $C_\infty$ of various polymers [3].

| Types of polymer | $M_e$ | $C_\infty$ |
|---|---|---|
| Polyethylene (PE) | 1,390 | 6.8 |
| Polybutadiene (PBD) | 1,740 | 5.4 |
| Polymethylmethacrylate (PMMA) | 9,200 | 8.6 |
| Polyethylmethacrylate (PEMA) | 8,590 | 7.7 |
| Poly n-butylmethacrylate (P n-Bu MA) | 12,200 | 8.0 |
| Poly n-hexylmethacrylate (P n-Hex MA) | 33,800 | 11.2 |
| Poly n-octylmethacrylate (P n-Oct MA) | 47,500 | 10.0 |
| Poly n-dodecylmethacrylate (P n-Doc MA) | 155,000 | 13.4 |
| Polystyrene (PS) | 18,700 | 10.8 |

As can be seen from this formula (1.5), $M_e$ is closely associated with the flexibility of the molecule. The molecules having higher $C_\infty$, in other words, the molecules with poor flexibility, are supposed to have a higher $M_e$.

Let us take a look at Table 1.1. Polyethylene (PE), which has the simplest structure and no functional groups, has a lower $C_\infty$ and thus a lower $M_e$ of 1,390. The molecular entanglements begin and become a polymer at a molecular weight of even as low as 1,300. On the other hand, Pn-DocMA, which has a very bulky functional group, has a higher $C_\infty$ and thus quite high $M_e$ of 150,000. It is surprisingly seen that even at molecular weights above 100,000, the molecular entanglements do not begin and thus this molecule does not become a polymer yet.

Therefore, the answer to the question of at what molecular weight does a molecule become a polymer depends on the molecular structure, particularly the flexibility of the molecule.

### 1.1.2 Primary, Secondary, and Higher-ordered Structures

Polymers are linear molecules formed by the connection of one or more types of repeating units. Their properties are largely determined not only by the chemical structure of the monomers, but also by the bonding pattern and degree of polymerization as a result of the reaction of the monomers. The structure determined by these chemical bonds is called the primary structure of the polymer. As an example, let us consider the addition polymerization of vinyl monomers. The polymerization of monomers having conjugated double or triple bonds can also result in geometric isomerism related to the unsaturated bonds in the main chain, such as cis-trans isomers. Furthermore, in addition to these linear polymers, highly branched and/or three-dimensional network polymers also exist, which exhibit physical properties different from linear polymers composed of the same repeating units. Copolymers can also be obtained by the copolymerization of two or more types of monomers. Monomers in the case of copolymers are called comonomers. In this case,

depending on the comonomer sequence, the properties of the resulting copolymers can be varied completely.

Like this, even a single polymer can have a surprising variety of primary structures, and this primary structure has a great influence on the formation of structures on a larger scale. The spatial form of a single polymer chain in solution is called the secondary structure, which corresponds to the helical structure and $\beta$ structure seen in polypeptides and proteins as examples. Furthermore, the structure of an aggregate of polymer chains is called a higher-order structure or tertiary structure. Slight differences in primary structure are reflected in higher-order structures such as the polymer crystal morphology, crystallinity, and microphase separation structures.

The primary structure of a polymer is determined by chemical bonds and is formed by chemical reactions such as addition polymerization, condensation, and polyaddition. Though the primary structure is extremely important when discussing the subsequent secondary and higher-order structures, we will skip this topic in this book. There are many excellent textbooks available [4–10]. If you want to study it in more detail, please refer to the references. In this book, we will start with the secondary structure and higher-order structure.

### 1.1.3 Secondary Structure

Many polymers contain C—C single bonds in their main chains. These C—C single bonds are capable of internal rotation. Because polymers have many rotatable bonds, the molecular chain can take on a variety of shapes as a result of the internal rotation, and the shape can be determined so as torsional potential to be minimized. This is one of the factors to determine the secondary structure of a polymer chain. Molecular chains that have different shapes due to internal rotation are called rotational isomers. The relative spatial arrangement of each atom or atomic group that arises from internal rotation is called a conformation.

Let us consider the rotation of the bond between $C_2$ and $C_3$ in n-butane, $C_4H_3—C_3H_2—C_2H_2—C_4H_3$. Figure 1.3 shows the Newman projection in which the $C_2—C_3$ axis is perpendicular to the paper.

The trans ($T$) form is the case where the bulkiest atomic groups attached to the adjacent rotating carbons are at the most far positions. $T$ is the most stable in terms of energy. Based on this state, the internal rotation potential energy is set to 0, and

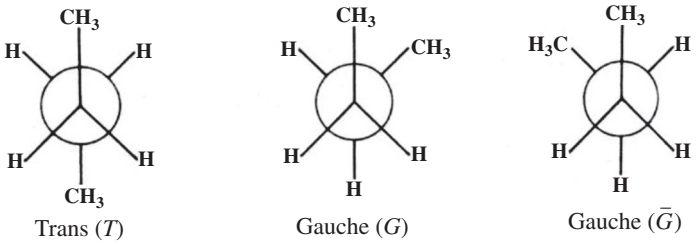


**Figure 1.3** Rotational isomer of n-butane, trans as $T$ and gauche as $G$ or $\bar{G}$.

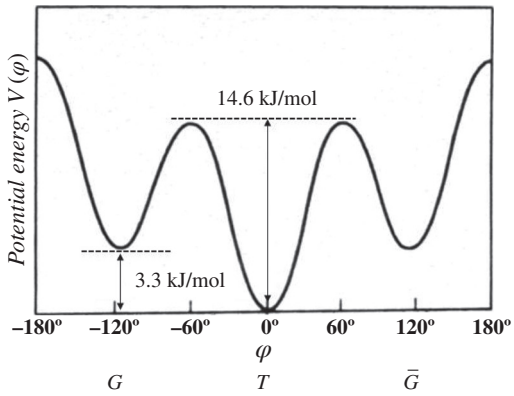


**Figure 1.4** Internal rotation angle $\varphi$ and corresponding internal rotation potential energy $V(\varphi)$ in n-butane.

the rotation angle is also set to be 0°. The gauche configuration ($G$ or $\overline{G}$) is the state where the bulkiest groups are rotated 120° clockwise or counterclockwise. This state is energetically the second most stable after the $T$ form. Figure 1.4 shows the relationship between the internal rotation angle and the corresponding potential energy $V(\varphi)$ in n-butane.

In Figure 1.4, the potential energy difference $T$ and $G$ or $\overline{G}$ is approximately 3.3 kJ/mol, while the potential barrier for overlapping two methyl groups (eclipsed) is 14.6 kJ/mol. Based on those values, let us estimate the conformation of n-butane at 27 °C. The thermal energy at 27 °C is RT = 2.5 kJ/mol, and the rotational frequency is in the infrared region, which is $\nu = 10^{13}$/s. We can calculate the frequency $N$ using the following formula (1.6) when $G \leftrightarrows \overline{G}$ transformation which needs to overcome the highest potential barrier.

$$N = \nu \exp\left(-{}^{\Delta U}\!/_{RT}\right) \tag{1.6}$$

Inserting 14.6 kJ/mol as $\Delta U$, $10^{13}$/s as $\nu$ and 2.5 kJ/mol as $RT$ in this formula yields $3 \times 10^{10}$/s. It means that even with this level of potential barrier, the C—C bonds rotate freely.

In the case of polymers, it is assumed that larger atomic groups are joined around the rotating bonds, and thus the rotation is supposed to be, to some extent, restricted due to steric hindrance and increased mass of such larger atomic groups. However, NMR and viscoelasticity measurements reveal that fairly fast internal rotation still occurs in polymer solution or molten state.

Let us explain the pentane effect. As the molecular weight of a polymer increases and thus its molecular chain becomes longer, it becomes clear that not all the rotations are permitted. We will explain this using n-pentane as an example. A n-pentane should originally have $3^4 = 81$ rotational isomers. Yet, when $C_2$—$C_3$ bond and $C_3$—$C_4$ bond rotate, they correspond to $G\overline{G}$ and $\overline{G}G$ conformation, respectively. In this case, the hydrogen atoms bonded to $C_5$ get very close to each other, as shown in Figure 1.5. A strong repulsive force works, which causes an increase in the potential energy, thus making the probabilities of those conformations extremely low. This effect is called the short-range interaction, the four-bond interaction, or the pentane effect.

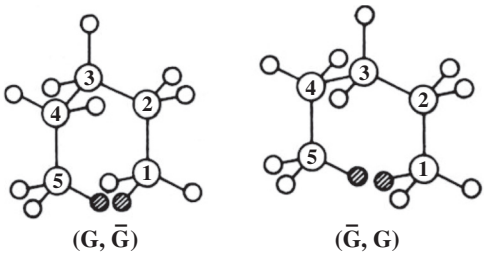


**Figure 1.5** Four-bond interaction of n-pentane.

When considering longer molecular chains, parts of the molecular chain spatially expanding due to repeated internal rotations may return and overlap each other. In this case, parts of the molecules that are quite far apart along the molecular chain interact with each other, which is called the long-range interaction or the excluded volume effect. This effect becomes more pronounced as the molecular chain becomes longer.

Like these effects, in the secondary structure of a polymer with such long chains, there is a certain restriction on the degree of structural flexibility.

In addition to structural control through the internal rotation, other interactions related to the determination of secondary structure include electrostatic interactions between ionic polymers or between ionic polymers and their counter ions, which are prominent in polymer electrolytes, hydrogen bonds that play an important role in biopolymers and polyamides, and dipole-dipole interactions when polar groups are included in the polymer chain.

### 1.1.4 Higher-order Structure

Higher-order structure or tertiary structure is defined as the structure of an assembly of molecular chains formed as a result of their intermolecular interactions. For example, polymer crystals, amorphous structures, and liquid crystal structures correspond to this category. Spherulite structures formed by the assembly of polymer crystals, and the microphase separation seen in block copolymers by the combination of secondary and tertiary structures are included in this category.

First, let us explain the higher-order structure of semi-crystalline polymers. Even crystalline polymers do not have 100% crystallinity, and thus always contain some portion of amorphous parts, which greatly affect their physical, mechanical, and thermal properties. In terms of thermal properties, the thermal expansion, the main theme of this book, is also greatly influenced by the thermal expansion of the amorphous portion. The thermal expansion phenomenon of the amorphous portion of semicrystalline polymers and amorphous polymers is explained in detail in Chapter 2 using the free volume theory.

Figure 1.6 is a schematic diagram of an amorphous region sandwiched between stacks of polymer crystals (called lamellae). When a polymer crystallizes from a melt, polymer chains are packed into a crystal lattice, but the entanglements of polymer chains present in the melt are excluded from the crystal. Hence, the amorphous region sandwiched between stacked lamellar crystals is thought to

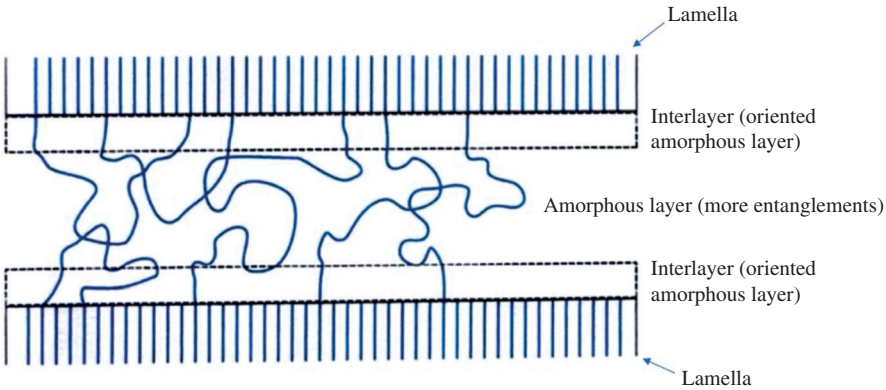


**Figure 1.6** Amorphous region sandwiched between lamellar crystals.

have more entanglements than the bulk amorphous state. However, due to the fact that the length of a single polymer chain is significantly longer than the thickness of the lamellar crystals, the polymer chains protrude from the lamellar crystals into the amorphous phase. Right after the protrusion, the polymer chains retain their orientation in the crystal and thus are oriented perpendicular to the lamellar layers. This is thought to have a different structure from the amorphous phase in the bulk. This oriented amorphous phase, which is neither crystalline nor completely amorphous, is sometimes called an interlayer.

Polymers are processed into final products by injection molding, extrusion molding, etc. During these processes, the molecular chains become oriented along the flow direction. In this process, polymer molecules are oriented in the flow direction and solidify within the mold. In crystalline polymers, amorphous molecules also become oriented as crystalline lamellae are formed. The amorphous molecules that connect the lamellae are highly oriented, and some of them are called tie molecules. The presence of tie molecules has a significant effect on the mechanical and thermal properties of the product. A morphology model of oriented PE is shown in Figure 1.7 [11].

From here, we will explain the crystal structures of some representative crystalline polymers that are frequently cited in this book, but before that, we would like to briefly review the fundamentals of polymer crystal lattice. The crystal lattice of polymers is no different from that of small molecules or metals. A unit called a unit cell exists in a crystal, and the entire crystal is formed by its translational displacement. Generally, a unit cell is a parallelepiped, and is defined by the lengths of its three axes ($a$, $b$, $c$) and the angles ($\alpha$, $\beta$, $\gamma$) between them (Figure 1.8).

The unit cell is classified into seven crystal systems: triclinic, monoclinic, orthorhombic, trigonal, tetragonal, hexagonal, and cubic. Table 1.2 shows the details of those seven crystal systems. The $c$-axis is often used as the molecular growth axis.

Such crystalline structures are greatly influenced by the primary and secondary structures of a polymer. Whether or not a polymer will crystallize depends on its primary structure, that is, the molecular chain must first have stereoregularity,

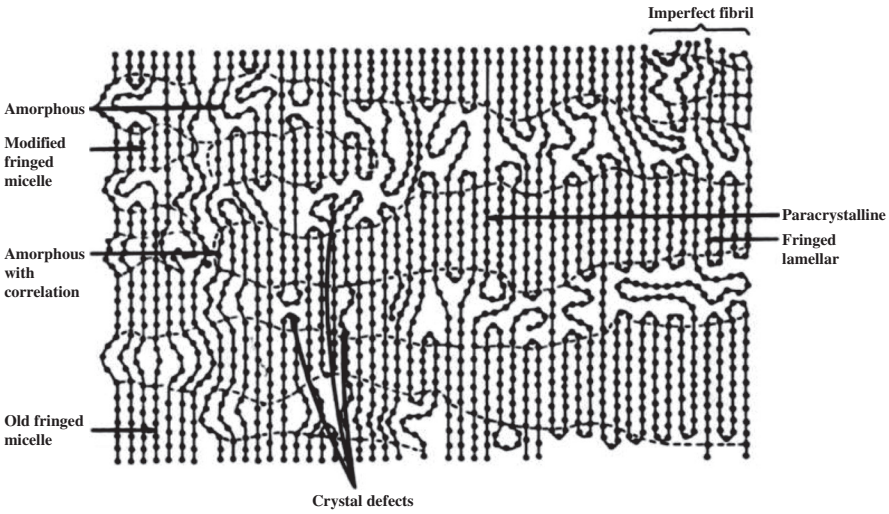


**Figure 1.7** Schematic diagram of different types of order and disorder in an oriented semicrystalline polymer [11].

and a short side chain and good symmetry also have an influence on high crystallinity. With regard to the actual crystalline structure, the secondary structure determines the periodicity in the molecular chain direction, while van der Waals forces between molecules determine the intermolecular distance. In polymers that have hydroxyl groups in the molecular chain, such as nylon and polyvinyl alcohol (PVA), hydrogen bonds also affect the crystalline structure.

The theoretical potential energy of a crystal is calculated taking into account internal rotational potentials, nonbonded atomic interactions, electrostatic interactions, and in some cases hydrogen bonding.

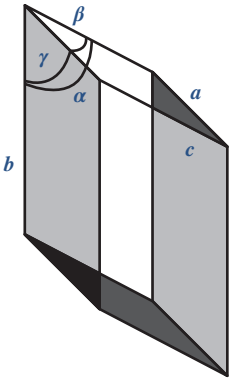


**Figure 1.8** Definition of each axis and angle in a unit cell.

The internal rotational potential $V(\varphi)$ is expressed as

$$V(\varphi) = \frac{1}{2}V_0(1 - \cos 3\varphi) \tag{1.7}$$

where $\varphi$ is internal rotational angle and $V_0$ is the height of the potential barrier of internal rotational potential. The $V_0$ is expressed as the formula (1.8) using force constant $f$, bond length $l$, and bond angle $\theta$.

$$V_0 = \frac{2}{9}l^2 f \sin^2\theta \tag{1.8}$$

The nonbonded atomic interaction $V_{ij}$ is expressed as the formula (1.9) using the Lennard-Jones 6–12 potential.

$$V_{ij} = 4\varepsilon_{ij}\left\{\left(\frac{\sigma_{ij}}{r_{ij}}\right)^{12} - \left(\frac{\sigma_{ij}}{r_{ij}}\right)^{6}\right\} \tag{1.9}$$

**Table 1.2** Crystal system.

| Crystal System | Axis | Angle |
|---|---|---|
| Triclinic | $a \neq b \neq c$ | $\alpha \neq \beta \neq \gamma$ |
| Monoclinic | $a \neq b \neq c$ | $\alpha = \gamma = 90° \neq \beta$ |
| Orthorhombic | $a \neq b \neq c$ | $\alpha = \beta = \gamma = 90°$ |
| Trigonal | $a = b = c$ | $\alpha = \beta = \gamma < 120° (\neq 90°)$ |
| Tetragonal | $a = b \neq c$ | $\alpha = \beta = \gamma = 90°$ |
| Hexagonal | $a = b \neq c$ | $\alpha = \beta = 90°, \gamma = 120°$ |
| Cubic | $a = b = c$ | $\alpha = \beta = \gamma = 90°$ |

where $\varepsilon_{ij}$ and $\sigma_{ij}$ are the parameters determined by the type of atom, where $\varepsilon_{ij}$ is the depth of the potential well and $\sigma_{ij}$ is one of the values of the interatomic distance $r_{ij}$ at which $V_{ij} = 0$.

The electrostatic interaction $V_{\text{electro}}$ is generated by the interactions between dipoles. If we assume that formal charges are placed at the positions of each atom relative to the dipole moment and use a point charge model to represent electrostatic interactions with their Coulomb potentials, the electrostatic interaction is expressed as the formula (1.10)

$$V_{\text{electro}} = \frac{q_i q_j}{\mu r_{ij}} \tag{1.10}$$

where $q_i$ and $q_j$ are the $i$-th and $j$-th formal charges, and $\mu$ is the dielectric constant.

Now, let us consider a crystal consisting of $N$ molecular chains. The entire crystal energy $V_{\text{crystal}}$ is expressed as the sum of the intramolecular and intermolecular interactions, as follows:

$$V_{\text{crystal}} = NV_{\text{intra}} + \sum_{n=1}^{N-1} \sum_{n'>n}^{N} V_{\text{inter}}(n; n') \tag{1.11}$$

where $V_{\text{intra}}$ is the intramolecular interaction of one polymer chain, and $V_{\text{inter}}(n; n')$ is the intermolecular interaction between the $n$-th and $n'$-th molecules.

The $V_{\text{intra}}$ is considered as the sum of the potential energy due to intramolecular rotation and the potential energy due to the $u$-th and $u'$-th dipoles of a single chain and van der Waals interactions. If a chain is assumed to be composed of $M$ atoms and the number of bonds in the main chain that can be internally rotated is $P$, the following formula is obtained:

$$V_{\text{intra}} = PV_{\text{rot}} + \frac{1}{2} \sum_{u=0}^{M} \sum_{u'=0}^{M} V_{\text{intra}}(u; u') \tag{1.12}$$

The minimum value of $V_{cr}$ is determined using $r_{ij}$ as a variable. The resulting $r_{ij}$ and $V_{cr}$ are the theoretically determined values of the crystal. Calculations using the formula (1.11) are applied to many crystalline polymers, such as PE, polyvinylidene fluoride, and polypropylene (PP), by which the shape of the molecular chain in the crystal lattice and the setting angle between the crystal axis and the molecular chain are determined.

The above-mentioned concepts can be used to explain the crystalline structures of polymers. Next, we will introduce the crystalline structures of some representative polymers that appear in this book.

#### 1.1.4.1 Polyethylene

The crystal structure of PE is shown in Figure 1.9. PE is most stable as a single molecular chain when each bond is in the trans position. This conformation is flat, so it is called a planar zigzag structure. The crystal has an orthorhombic crystalline form with $a$-axis of 7.40 Å, $b$-axis of 4.93 Å, and $c$-axis of 2.53 Å. The molecular axis is oriented along the $c$-axis. There are two molecular chains in the unit cell, and the setting angle α between the planar zigzag chain of the central molecular chain and the $a$-axis is approximately 45°.

Let us calculate the crystalline density $\rho_c$ of PE using these lattice constants. If the molecular weight of the repeating unit is $M$, then there are two PE molecular chains in this unit cell, thus $\rho_c$ can be obtained as

$$\rho_c = \frac{2 \times M}{abc \times 10^{-24} \times A_v} = \frac{2 \times (28.054)}{7.40 \times 4.93 \times 2.534 \times 10^{-24} \times \left(6.025 \times 10^{23}\right)}$$
$$= 1.007 \text{ g/cm}^3$$

where $A_v$ is Avogadro's number.

The actual density of PE is around 0.940 g/cm$^3$, which is lower than the $\rho_c$. This means that crystallization does not perfectly occur.

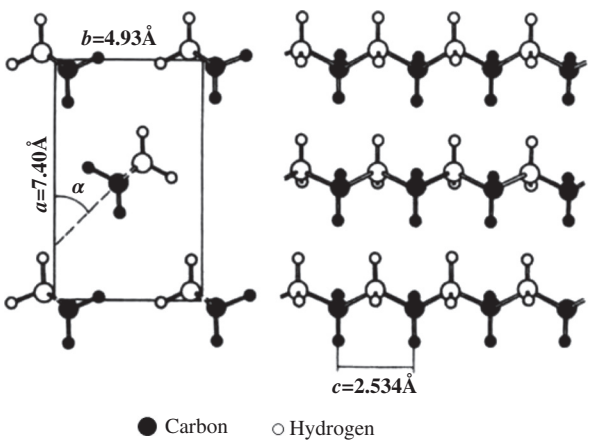


**Figure 1.9** Crystal structure of PE.

#### 1.1.4.2 Isotactic Polypropylene

There are three types of PP, namely isotactic PP (iPP), syndiotactic PP (sPP), and amorphous PP, which differ in the conformation of the methyl groups in the main chain. Here we will introduce the crystal structure of iPP, which is industrially important.

When the main chain conformation of iPP is changed to trans, the hydrogen atoms of the methyl groups in adjacent side chains come abnormally close to each other, resulting in a high-energy state known as the pentane effect. This results in *TGTG* conformation, with alternating trans and gauche conformations. The molecular chain forms a helix structure with three monomers, completing one full rotation. This structure is designated $3_1$. The iPP is known to have four types of crystal structures, α, β, γ, and liquid crystal, depending on the crystallization conditions.

The α-type is the most stable, and its crystal and molecular chain configuration are shown in Figure 1.10 [12]. The α-type has a monoclinic crystal form, with lattice constants of $a = 0.665$, $b = 2.096$, $c = 0.650$ nm, and $\beta = 99.2°$. The fiber period along the $c$-axis is 0.11 nm shorter than the period of the planar zigzag chain, 0.2534 nm, due to its helix structure. Furthermore, due to this helix structure, the diameter of the crystalline molecular axis is larger than that in the planar zigzag chain as shown in Figure 1.10(b). As a result, the $a$ and $b$-axes are longer and the crystalline density $\rho_c$ of 0.936 g/cm$^3$ than those of PE.

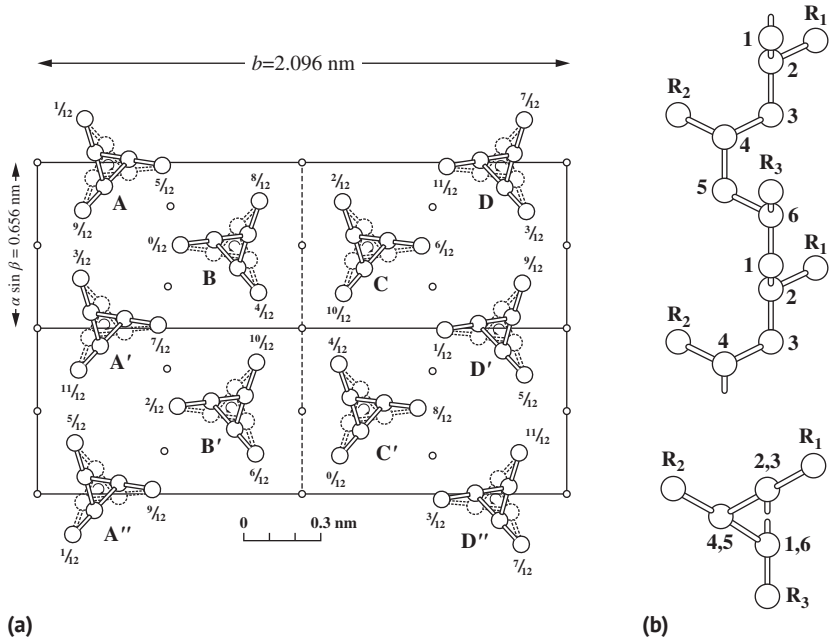


**Figure 1.10** Crystal structure (a) of isotactic polypropylene (b) and conformation of molecular chain [12].

#### 1.1.4.3 Nylon 6,6

Crystalline polymers in which intermolecular hydrogen bonds play an important role in the crystalline structure include polyamides, cellulose, PVA, and polyamino acids. Figure 1.11 shows the crystal structure of nylon 6,6, which is one of the industrially important polyamides [13].

The methylene chains rotate intramolecularly to form a trans-type planar structure. Therefore, nylon molecular chains have a planar zigzag conformation. Hydrogen bonds C═O····H—N are formed between molecules on the same plane in the $a$-axis direction, as shown by the dashed lines in Figure 1.11. In order to form hydrogen bonds, the molecular chains must shift one by one. In other words, the heights of the C═O····H—N bonds increase one by one. As the $a$, $b$, $c$-axes are not perpendicular to each other, the crystal system is a triclinic system. The lattice constants are $a = 0.49$, $b = 0.54$, $c = 1.72$ nm, $\alpha = 48.5$, $\beta = 76.5$, and $\gamma = 63.5°$. In this crystal, hydrogen bonds exist in the $a$-axis direction within the $ac$ plane, and bonds along the $b$-axis direction are formed by van der Waals forces. Thus, nylon molecular chains form a layered structure through hydrogen bonding. The overlapping of these layers creates a crystalline structure. The difference in the types of bond forces between $a$ and $b$-axes causes anisotropy in the intermolecular direction, and the non-hydrogen-bonded interlayer direction ($b$-axis direction) is weak, so it can easily peel off when subjected to external force.

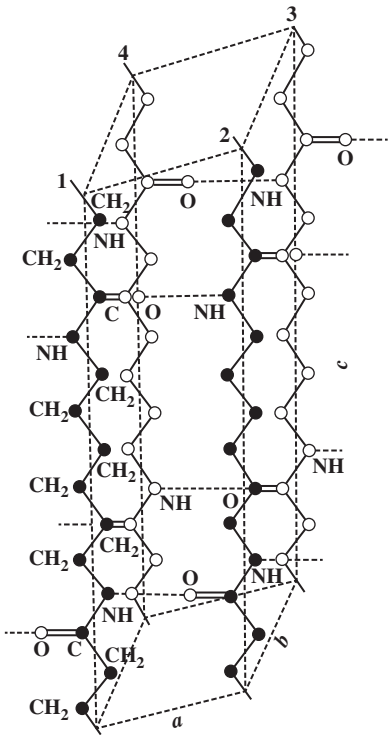


**Figure 1.11** Crystal structure of nylon 6,6 [13].

## 1.2 Polymer ABC, Alloy, Blend, and Composite

So far, we have introduced the basics of the structure of a single polymer. There are various methods for controlling the thermal expansion of polymer materials, the subject of this book. One of these is control by mixing with other materials. Specifically, this includes composites, which are mixed with fillers, and blends and alloys, which are mixed with other polymers. Specific methods are described in detail in Chapters 5 and 6 of this book. Here, we will briefly touch on the basics of polymer blends, alloys, and composites.

Let us explain polymer alloy and blend. To tell the truth, there is no clear borderline between polymer alloy and blend. If we would define polymer alloys as only

completely miscible systems in which the two polymers are mutually soluble at their molecular level at any compositions and at any temperatures, then there are almost few systems that can be called "polymer alloy" (polyphenylene ether (PPE)/PS alloy, called "Noryl™ resin" is known as one of such perfectly homogeneous alloys, but it is quite rare example [14]). This is because even in completely miscible system, most such systems have a so-called phase diagram in which phase separation occurs depending upon temperatures and compositions. Thus, in this book, we will ask readers for understanding that we will use the terms "polymer alloy" and "polymer blend" without making a distinction.

### 1.2.1 Interfaces in Polymer Alloy and Blend

Firstly, let us explain a polymer-polymer interface. When two types of polymers are mixed, unless they are a completely miscible alloy, phase separation occurs, and therefore an interface is inevitably generated.

At the interface of such a phase-separated polymer blend, the effect of different polymer chains mixing together to increase entropy and the effect of those repelling each other compete with each other, resulting in the generation of a certain thickness at the interface. It is shown in Figure 1.12 [15].

Cahn-Hilliard theory [16] is used to express the free energy of such an inhomogeneous concentration system. When the concentration changes slowly, the Helmholtz free energy of the system $\Delta F$ is given by

$$\Delta F = \int_V \left\{ \Delta f_m(\phi) + \kappa \left( \nabla \phi \right)^2 \right\} dV / v_0 \tag{1.13}$$

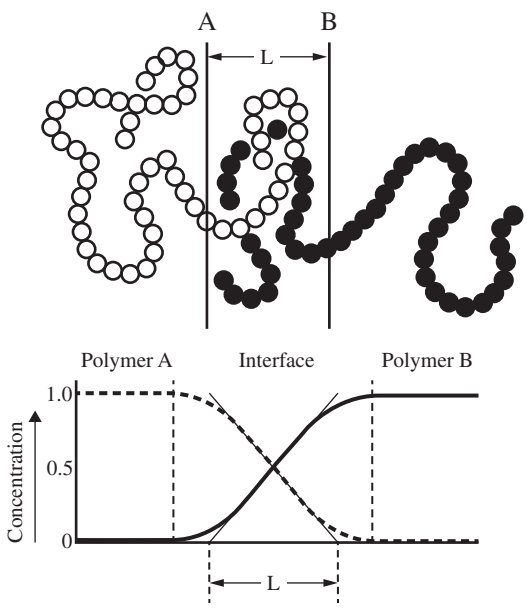


**Figure 1.12** Polymer chains and a concentration profile image at the interface [15].

where $\Delta f_m(\phi)$ is a term that depends on the local concentration $\phi$, the term of $\kappa(\nabla\phi)^2$ is the excess free energy due to the presence of the concentration gradient $\nabla\phi$, $\kappa(>0)$ is a coefficient when the second-order expansion term is taken, and $v_0$ is the lattice volume. If the free energy when there is no interface is $\Delta f_0$ and $\Delta f = \Delta f_m - \Delta f_0$, the interfacial tension $\tau$ is given by

$$\tau = \int_{-\infty}^{\infty} \left\{ \Delta f(\phi) + \kappa \left( \frac{\partial \phi}{\partial z} \right)^2 \right\} dz/v_0 \tag{1.14}$$

The condition for equilibrium is that the interfacial tension $\tau$ is minimized, which gives the formula (1.15) based on Euler's theorem.

$$\Delta f(\phi) = \kappa \left( \frac{\partial \phi}{\partial z} \right)^2 \tag{1.15}$$

Inserting the formula (1.15) into the formula (1.14) yields the formula (1.16).

$$\tau = \left( \frac{2}{v_0} \right) \int_{-\infty}^{\infty} \Delta f(\phi) dz = \left( \frac{2}{v_0} \right) \int_{\phi'}^{\phi''} (\kappa \Delta f(\phi))^{1/2} d\phi \tag{1.16}$$

where $\phi'$ and $\phi''$ are the coexisting concentration ($\phi'' > \phi'$).

The thickness of the interface $L$ is given by

$$L = \frac{(\phi'' - \phi')}{(d\phi/dz)_{\max}} = \Delta\phi \left( \frac{\kappa}{\Delta f(\phi)} \right)_{\max}^{1/2} \tag{1.17}$$

It is noteworthy here that the equilibrium of the interface is determined by the balance between the free energy term and the energy gradient term.

If $\Delta f(\phi)$ and $\kappa$ are given as a function of $\phi$, $\tau$, and $L$ can be numerically determined. As for $\Delta f_m(\phi)$, the following formula (1.18) obtained from the Flory-Huggins mean field approximation can be utilized:

$$\frac{\Delta f_m}{kT} = \frac{\phi_A}{N_A} \ln \phi_A + \frac{\phi_B}{N_B} \ln \phi_B + \chi \phi_A \phi_B \tag{1.18}$$

where $N_i$ is the degree of polymerization, and $\chi$ is the interaction parameter between polymers $A$ and $B$, and it decreases as the interaction between polymers increases. The Flory-Huggins equation will be explained in more detail in the next section (C).

In the case of a polymer-polymer system, since $N_i$ is large, the first and second terms can be almost ignored, and only the third term needs to be considered.

In terms of $\kappa$, it is necessary to consider the $\kappa$ separately as the contribution of enthalpy ($\kappa_e$) and the contribution of entropy ($\kappa_s$). Nose derived the following formula [17, 18]:

$$\kappa = \kappa_e + \kappa_s = \frac{\chi l^2}{2} + \left( \frac{{a_A}^2}{36\phi_A} + \frac{{a_B}^2}{36\phi_B} \right) \tag{1.19}$$

where $l$ is the interaction distance (e.g., Debye distance), and $a_i$ is the segment length.

The $\kappa_e$ corresponds to the change in contact energy due to the energy gradient. On the other hand, when there is a concentration gradient, the entropy of the polymer chain configuration cannot be expressed in the form of the Flory-Huggins equation. This is reflected in $\kappa_s$.

Based on these, $\tau$ and $L$ have been calculated using various approximations. Here, we introduce the results obtained using a statistical mechanical method based on the self-independent field theory by Helfand and Tagami [19, 20].

$$\tau = \left(\frac{\chi}{6}\right)^{1/2}\left(\frac{kT}{v_0}\right)a \tag{1.20}$$

$$L = \left(\frac{2}{\sqrt{6}}\right)a\chi^{-1/2} \tag{1.21}$$

For this calculation, $a_A = a_B = a$ and $N_A = N_B = N$.

Looking at the formula (1.21), it is found that the interfacial thickness $L$ is proportional to $\chi^{-1/2}$. In other words, as the interaction between polymers becomes stronger, thus its $\chi$ decreases, the interfacial thickness $L$ increases.

The density distribution of polymers A and B at the distance $z$ from the interface, with the interface as the origin, is also calculated.

$$\frac{\rho_A(z)}{\rho_0} = \frac{1}{1 + \exp\left(-\frac{2\sqrt{6\chi}z}{a}\right)} \tag{1.22}$$

$$\frac{\rho_B(z)}{\rho_0} = \frac{1}{1 + \exp\left(\frac{2\sqrt{6\chi}z}{a}\right)} \tag{1.23}$$

Let us use the formulas (1.20) and (1.23) to calculate $\tau$, $L$, and density distribution for actual polymer system. Let us consider PS/polymethylmethacrylate (PMMA) at $T = 140$ °C. In this blend, each segment length is 0.66 nm of $a_{PS}$ and 0.64 nm of $a_{\mathrm{PMMA}}$, respectively. We will take the average of them, which is 0.65 nm as $a$. The density of each is 0.0102 mol/cm$^3$ as $\rho_{\mathrm{PS}}$ and 0.0116 mol/cm$^3$ as $\rho_{\mathrm{PMMA}}$, respectively, and we will take the average of them, which is 0.109 mol/cm$^3$ as $\rho_0$. For this blend system, its $\chi$ was obtained as $\chi = 1.0 \times 10^{-2}$. Inserting those values into the formulas (1.20) and (1.23) yields $L = 5.3$ nm and $\tau = 1.0$ dyn/cm $= 1.0 \times 10^{-3}$ N/m. The value of this $\tau$ is close to the value experimentally obtained by Wu, 1.7 dyn/cm [21].

The result of the density distribution by the formulas (1.22) and (1.23) is shown in Figure 1.13.

At the end of this section, we will introduce the relationship between the dispersed particle size of a minor component in a phase-separated polymer blend and its interface. In phase-separated polymer blends, the particle size of the minor component has a significant effect on the physical properties of the final product. In particular, to control impact resistance, it is common to add a rubber component as a minor component and finely disperse it in the matrix polymer to improve impact resistance.

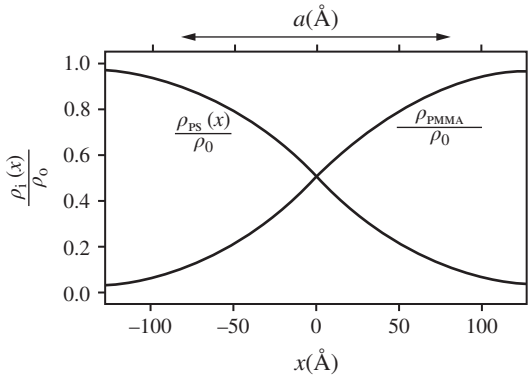


**Figure 1.13** Density distribution profile of PS/PMMA at 140 °C.

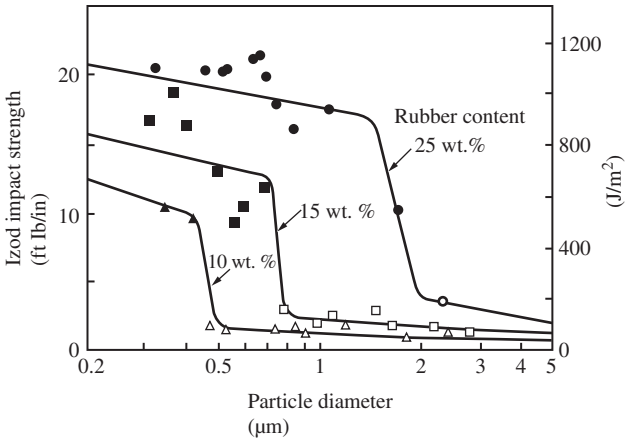


**Figure 1.14** Particle size and Izod impact strength of rubber-toughened nylon [22].

Figure 1.14 shows the relationship between rubber particle size and Izod impact strength for rubber-toughened nylon [22].

It can be seen that at any rubber content, a rapid transition from brittle to ductile fracture occurs below a certain rubber particle size. Like this, impact resistance is thus extremely sensitive to the particle size of dispersed rubber, and therefore requires precise control of it.

Here, let's look at the relationship between dispersed particle size and the interface. Eliminating $\chi$ from the formulas (1.20) and (1.21) gives the formula (1.24).

$$\tau = \left(\frac{kTa^2}{3v_0}\right)\left(\frac{1}{L}\right) \propto L^{-1} \tag{1.24}$$

When a polymer blend is prepared by melt blending with an extruder, the minimum dispersed particle size $d$ of the resulting dispersed component is expressed by the following formula (1.25):

$$d = \left(\frac{C\tau}{\eta_m \dot{\gamma}}\right) f\left(\frac{\eta_d}{\eta_m}\right) \tag{1.25}$$

where $C$, $\eta_d$, $\eta_m$, and $\dot{\gamma}$ are a constant, melt viscosity of the minor component, melt viscosity of the major component, and shear rate in an extruder, respectively.

Based on the formulas (1.24) and (1.25), we can obtain:

$$d \propto \tau \propto L^{-1} \tag{1.26}$$

It can be seen that the dispersed particle size is proportional to the interfacial tension $\tau$, and thus inversely proportional to the thickness of the interface $L$. This means that the thicker the interface, the finer the dispersed particle size can be. We hope you now understand how important the control of the interface is to control the interface.

### 1.2.2 Phase Diagram and Flory-Huggins Theory

As mentioned in (A), when two or more polymers are arbitrarily selected and mixed, in most cases they will be phase-separated. However, to date, several hundred miscible systems have been discovered. Of those miscible polymer systems, there are very few so-called completely miscible systems that are miscible at all compositions and temperatures (as introduced in (A), Noryl™ resin consisting of PPE/PS alloy is one of such systems), and in most cases, the phase diagram shows that the materials are miscible or phase-separated depending on the conditions.

Here we will introduce some examples of typical phase diagrams. Figure 1.15 shows the phase diagram for a PS/polybutadiene (PBD) mixture, which is an example of an upper critical solution temperature (UCST) type phase diagram, where phase separation occurs at low temperatures and the mixture becomes miscible as the temperature increases [23]. Both PS and PB are oligomers with molecular weights of several thousand. The UCST-type phase diagrams are often seen in blend systems where oligomers are contained.

Figure 1.16 shows the phase diagram of the PS/polyvinyl methyl ether (PVME) mixture [24]. In this type of phase diagram, when the temperature is lowered, the mixture becomes miscible, and when the temperature is raised, the mixture separates. Since there is a lower limit temperature for phase separation, it is called a lower critical solution temperature (LCST) type phase diagram. Although it may be difficult to accept this phenomenon intuitively, in fact, the majority of phase diagrams discovered to date are LCST-type phase diagrams. LCST-type phase diagrams are often seen in blends of high molecular weight polymers.

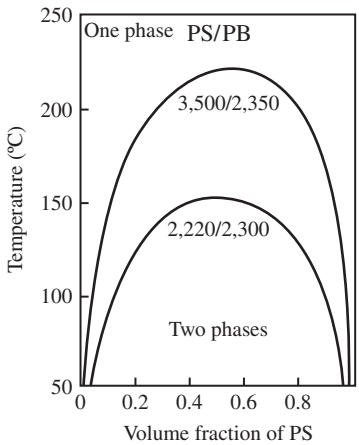


**Figure 1.15** USCT-type phase diagram of PS/PB mixture [23].

Furthermore, there are some blends in which both LCST and UCST-phase diagrams coexist, and when a blend of a given composition is heated, it changes from a phase-separated ~ a miscible ~ phase-separated systems. The phase

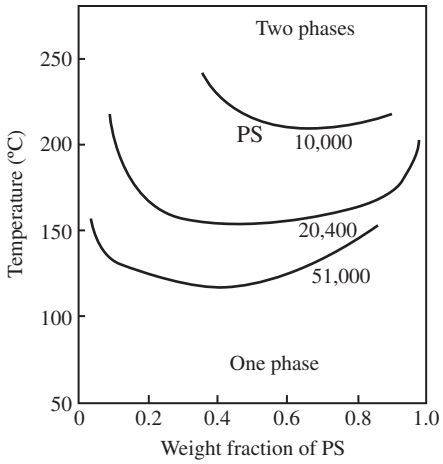


**Figure 1.16** Phase diagram of PS/PVME mixture as an example of LCST-type phase diagram [24].

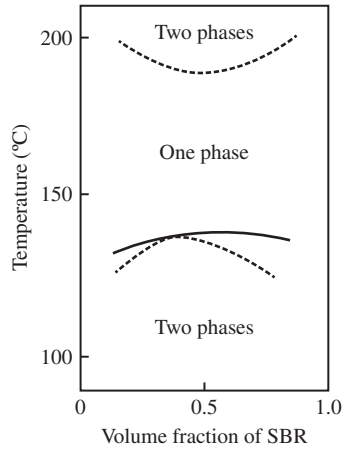


**Figure 1.17** Phase diagram of PS/SBR [25].

diagram of the PS/polystyrene-polybutadiene copolymer (SBR) blend as one of such examples is shown in Figure 1.17 [25].

Many studies are being conducted into the theoretical systematization of polymer-polymer miscibility, including the interpretation of these phase diagrams. Basically, it is sufficient to deal with the state of a system at a constant temperature $T$ and constant pressure $P$. If the free energy of mixing $\Delta G_{mix}$, that is, the change in free energy before and after mixing, is described as a function of the parameters to express polymer systems, such as mixture composition, temperature, and molecular weight, it becomes possible to quantitatively discuss whether different molecules will dissolve in each other, and even the shape of the phase diagram.

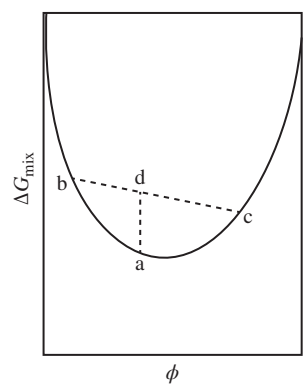


**Figure 1.18** $\Delta G_{mix}$ of polymer-polymer mixture as a function of volume fraction $\phi$.

When there is no change in volume ($\Delta V_{mix} = 0$), the $\Delta G_{mix}$ associated with mixing can be expressed as follows using the enthalpy change $\Delta H_{mix}$ and entropy change $\Delta S_{mix}$ associated with mixing:

$$\Delta G_{mix} = \Delta H_{mix} - T\Delta S_{mix} \tag{1.27}$$

$\Delta G_{mix} < 0$ is the condition that two polymers are miscible. This will be explained using Figure 1.18. Let's assume the $\Delta G_{mix} - \phi$ ($\phi$: volume fraction) curve is as shown in Figure 1.18. When composition $\phi = a$ separates into two phases, $b$ and $c$, the free energy change $\Delta G_{mix}(d)$ is larger than $\Delta G_{mix}(a)$ when there is only one phase. This holds true for all compositions. Therefore, this system will not undergo phase separation.

In other words, the condition for miscibility $\Delta G_{mix} < 0$ is equivalent to satisfying the following equation:

$$\frac{\partial^2 \Delta G_{mix}}{\partial \phi^2} < 0 \tag{1.28}$$

We introduce the Flory-Huggins lattice model, which is the simplest and most representative theory for calculating $\Delta G_{mix}$ [26, 27]. We will introduce the Flory-Huggins theory, one of the simplest and most representative theories for calculating $\Delta G_{mix}$. In this theory, $\Delta S_{mix}$ is calculated using a lattice model like the one shown in Figure 1.19.

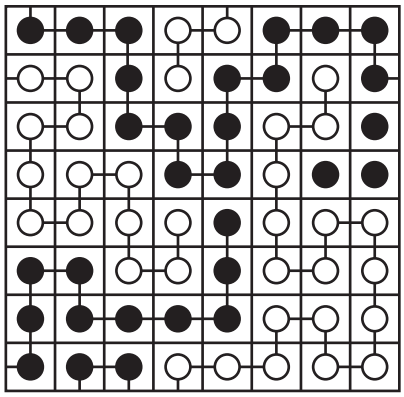

**Figure 1.19** Polymer-polymer mixture in a lattice.

It assumes that a polymer chain consists of $m_i$ segments, each arranged in a single lattice, and calculates the number of ways that polymer molecule 1 with a degree of polymerization of $m_1$ and polymer molecule 2 with a degree of polymerization of $m_2$ can be arranged on the lattice in $N_1$ and $N_2$ rows, respectively. Although details of the calculation of $\Delta S_{mix}$ are skipped here, the $\Delta S_{mix}$ can be obtained as follows:

$$\Delta S_{mix} = -k(N_1 \ln \phi_1 + N_2 \ln \phi_2) \tag{1.29}$$

where $\phi_1$ and $\phi_2$ are volume fraction of polymer 1 and 2, respectively. $\phi_1$ and $\phi_2$ can be rewritten using $N_i$ and $m_i$ $(i = 1, 2)$ as follows:

$$\phi_1 = \frac{N_1 m_1}{N_1 m_1 + N_2 m_2} = \frac{N_1 m_1}{N_0} \tag{1.30}$$

$$\phi_2 = \frac{N_2 m_2}{N_1 m_1 + N_2 m_2} = \frac{N_2 m_2}{N_0} \tag{1.31}$$

where $N_0$ is the total number of segments, and thus $N_0 = N_1 m_1 + N_2 m_2$.

When $N$ is the number of moles of the segment, and $A_V$ is Avogadro's number, the formulas (1.30) and (1.31) are rewritten as

$$\phi_1 = \frac{N_1 m_1}{N_0} = \frac{N_1 m_1}{N A_V} \tag{1.32}$$

$$\phi_2 = \frac{N_2 m_2}{N_0} = \frac{N_2 m_2}{N A_V} \tag{1.33}$$

Using the formulas (1.32) and (1.33), $N_1$ and $N_2$ are rewritten as follows:

$$N_1 = \frac{N A_V}{m_1} \phi_1 \tag{1.34}$$

$$N_2 = \frac{N A_V}{m_2} \phi_2 \tag{1.35}$$

Inserting the formulas (1.34) and (1.35) into the formula (1.29) yields

$$\begin{aligned}\Delta S_{\text{mix}} &= -k(N_1 \ln\ \phi_1 + N_2 \ln\ \phi_2) = -k\left(NN_A\frac{\phi_1}{m_1}\ln\ \phi_1 + N_A\frac{\phi_2}{m_2}\ln\ \phi_2\right)\\ &= -NR\left(\frac{\phi_1}{m_1}\ln\ \phi_1 + \frac{\phi_2}{m_2}\ln\ \phi_2\right)\end{aligned} \tag{1.36}$$

where $R$ is the gas constant.

Moreover, let us consider $\Delta H_{\text{mix}}$. In the lattice model, if the energy involved in contact is $\omega$ (per molecule) and the coordination number is $z$, the number of two polymers that can approach each other is

$$\frac{N_1N_2m_1m_2(z-2)}{N_1m_1 + N_2m_2} \tag{1.37}$$

Thus, $\Delta H_{\text{mix}}$ is

$$\Delta H_{\text{mix}} = \frac{N_1N_2m_1m_2(z-2)\omega}{N_1m_1 + N_2m_2} \tag{1.38}$$

Here, we define the interaction parameter of $\chi$ as

$$\chi = (z-2)\frac{\omega}{kT} \tag{1.39}$$

Inserting the formulas (1.34), (1.35), and (1.39) into the formula (1.38) yields

$$\Delta H_{\text{mix}} = kTA_VN\chi\phi_1\phi_2 = NRT\chi\phi_1\phi_2 \tag{1.40}$$

If the molar volume of the segment in the system is $V_r$,

$$N = \frac{V}{V_r} \tag{1.41}$$

Inserting the formulas (1.36) and (1.40) into the formula (1.27), we can obtain the final form of $\Delta G_{\text{mix}}$ as

$$\begin{aligned}\Delta G_{\text{mix}} &= NRT\chi\phi_1\phi_2 + NRT\left(\frac{\phi_1}{m_1}\ln\ \phi_1 + \frac{\phi_2}{m_2}\ln\ \phi_2\right)\\ &= \frac{RTV}{V_r}\left(\frac{\phi_1}{m_1}\ln\ \phi_1 + \frac{\phi_2}{m_2}\ln\ \phi_2 + \chi\phi_1\phi_2\right)\end{aligned} \tag{1.42}$$

$g$ is defined as below formula (1.43), and the compatibility and phase separation of polymers 1 and 2 can be discussed based on the behavior of $g$.

$$g \equiv \frac{\Delta G_{\text{mix}}}{NRT} = \frac{\phi_1}{m_1}\ln\ \phi_1 + \frac{\phi_2}{m_2}\ln\ \phi_2 + \chi\phi_1\phi_2 \tag{1.43}$$

Here, we will explain why the two typical phase diagram types, USCT and LCST, shown in Figures 1.15 and 1.16, occur. The condition for the mixture of polymer 1, 2 to be stable without phase separation is that the second derivative of $g$ should be positive (see the formula (1.28)).

$$g'' = \frac{\partial^2\left(\frac{\Delta G_{\text{mix}}}{NRT}\right)}{\partial {\phi_1}^2} = \frac{1}{m_1\phi_1} + \frac{1}{m_2\phi_2} - 2\chi > 0 \tag{1.44}$$

$\chi$ is approximated by the following formula using the solubility parameters $\delta_1$ and $\delta_2$ of corresponding polymers 1 and 2. From here, to emphasize that $\chi$ is the interaction parameter between polymers 1 and 2, we will rewrite it as $\chi_{12}$.

$$\chi_{12} \cong \frac{1}{RT}(\delta_1 - \delta_2)^2 \tag{1.45}$$

The first two terms on the left side of the formula (1.44) are always positive, and in the formula (1.45), $\chi_{12} \geq 0$. If the temperature change of the formula (1.44) is shown in Figure 1.20(a), $g''$ becomes positive above a certain temperature $T_U$, and as $m_1$ and $m_2$ increase, $T_U$ shifts to higher temperatures. This explains the behavior of the UCST-type in Figure 1.15. However, this idea cannot explain the LCST-type phase diagram shown in Figure 1.16.

One of the theories to explain the LCST-type phase diagram is the equation of state theory [28–30]. Several theories have been proposed depending on the types of models constructed. For example, if the new Flory theory is extended to polymer systems by incorporating the free volume effect, $\chi_{12}$ becomes as follows [28]:

$$\chi_{12} \cong \frac{(-U_1)}{RT}\frac{X_{12}}{P_1^*} + \frac{C_{P,1}}{2R}\left(1 - \frac{T_1^*}{T_2^*}\right)^2 \tag{1.46}$$

where $U_1$ is the energy due to the configuration of polymer 1, $C_{P,1}$ is the specific heat at constant pressure of polymer 1, and $X_{12}$ is the interaction energy, expressed as follows:

$$X_{12} = \frac{q_1}{2m_1 v_{\text{seg}}^*}(\varepsilon_{11} + \varepsilon_{22} - 2\varepsilon_{12}) \tag{1.47}$$

where $v_{\text{seg}}^*$ is the occupied volume per unit segment, $\varepsilon_{ij}(i,j = 1,2)$ is the interaction potential energy between segments $i$ and $j$, $q_1$ is the surface area of polymer 1, and

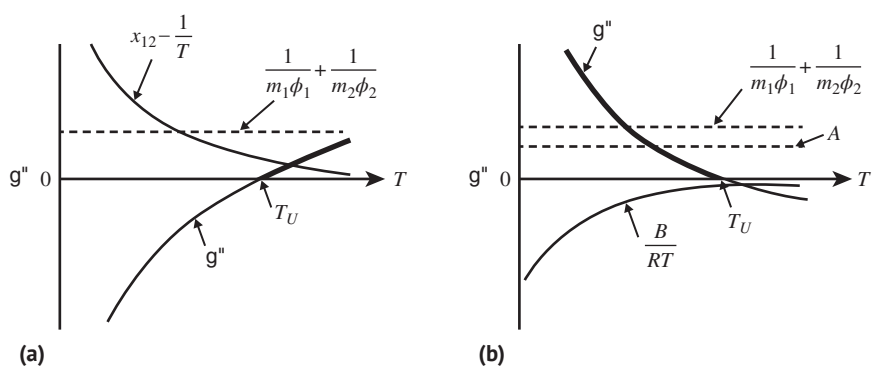


**Figure 1.20** Change in temperature of the second derivative of $g$: UCST (a) and LCST (b) type phase diagrams.

$P_i^*$ and $T_i^*$ are the characteristic pressure and characteristic temperature of polymer $i(i = 1, 2)$, respectively.

The first term in the formula (1.46) corresponds to a refinement of the formula (1.45), and this time it can take a negative value depending on whether $X_{12}$ is positive or negative. The second term is always positive and is zero for polymers where $T_1^*$and $T_2^*$ are equal. In addition, when the molecular motion of the polymer sufficiently occurs, $C_{P,1}$ has little temperature dependence, thus the second term can be considered to be approximately a constant. Thus, it can be simplified as

$$\chi_{12} \cong \frac{B}{RT} + A \tag{1.48}$$

where $A \geq 0$ and $B$ can take either a positive or negative value.

This is illustrated in Figure 1.20(b). When $B < 0$, $g''$ becomes positive below a certain temperature $T_U$ and becomes negative above that temperature. As $m_1$ and $m_2$ increase, $T_U$ shifts to the lower temperature side.

### 1.2.3 Polymer Composite

At the end of this chapter, we will touch on polymer composites. The polymer composites are the mixtures of polymers and inorganic or organic fillers. The size of the fillers used varies from millimeters (mm) down to nanometers (nm). The composites containing millimeter-sized fibers are, in particular, fiber-reinforced composites. The size of fillers that is commonly used is a few micrometers ($\mu m$). The composites with nanometer-sized fillers are called nanocomposites, and the unique surface effect from nano-dispersed fillers brings unique properties. One of such unique properties is the thermal expansion behavior, which is the subject of this book. This will be explained in Chapter 6.

In addition to the particle size of filler, the shape of it is also one of the factors to have significant influence on the final performance of the composite. The shapes can be roughly divided into spherical, fibrous, and flaky. Representative fillers belonging to each shape are shown in Figure 1.21.

The expected performance of composites by the addition of fillers is summarized in Figure 1.22. As seen in this chart, you can see that a wide variety of performance improvements can be expected to be brought. The thermal expansion control, which is the theme of this book, is also a performance affected by the filler addition. The relationship between filler shape, filler particle size, and thermal expansion is described in detail in Chapter 5.

Usually, the relationship between the performance of the composite and parameters of filler is described by the composite models, representing the Takayanagi model. Of course, we will introduce various types of the composite models let alone in Chapter 5 in this book as well. We will avoid the duplication of the introduction of such composite models here. Instead, in this chapter, we will explain polymer composites from a completely different perspective, which is the interaction between a polymer chain and filler surface.

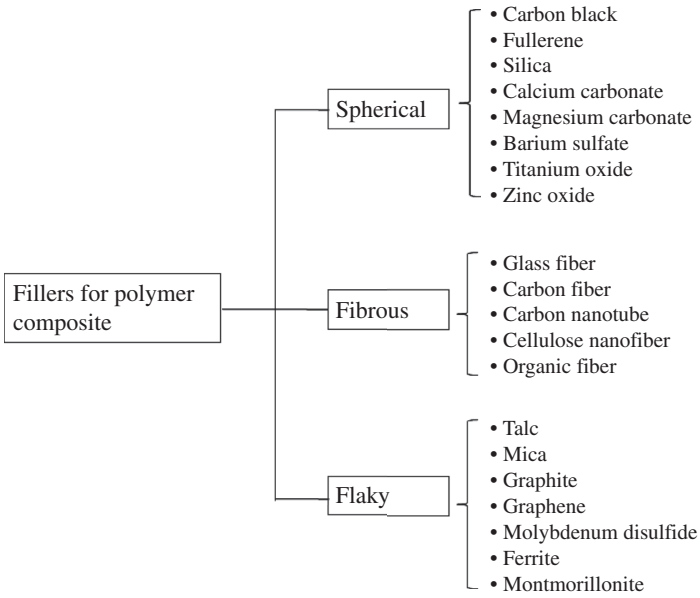


**Figure 1.21** Classification of fillers for polymer composites.

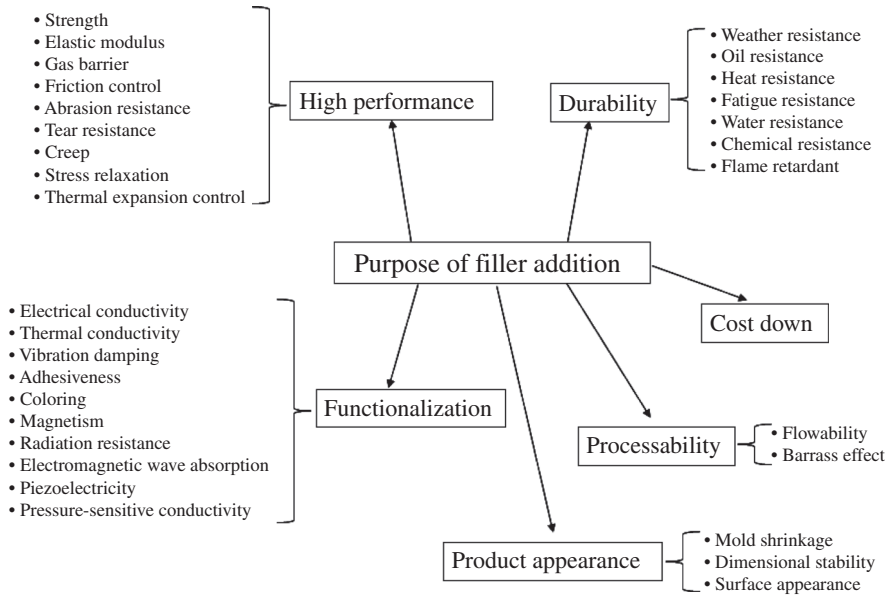


**Figure 1.22** Expected performance of composite materials by the addition of fillers.

We consider a model where a polymer chain is adsorbed onto the filler surface. The filler surface actually has a complex shape, but here we assume it is a smooth plane. The polymer chain is assumed to be a single chain in a dilute solution, and

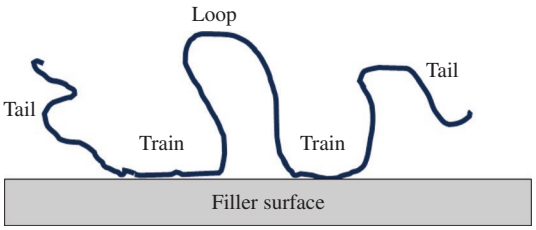


**Figure 1.23** Adsorption model of a polymer chain onto the plane filler surface: loop-train-tail model.

it is adsorbed onto the plane filler surface. The ultimate goal is to determine the thickness $t$ and density distribution $\phi(z)$ of the polymer chains on the filler surface.

In this case, some parts of the polymer chain are adsorbed onto the surface as a result of strong interaction with the surface, while other parts are able to move freely. This is shown schematically in Figure 1.23. This model is called the "loop-train-tail" model, where the train is segments of a chain adsorbed on the surface, the loop is segments of a chain that is bound at both ends by the trains but is located away from the surface, and the tail is segments of a chain with ends moving freely [31].

Now, let's consider a single polymer chain whose occupancy is restricted by an interface (wall). In this case, no segments are located on the other side of the wall, so its conformational entropy is reduced compared to the random coil state. Therefore, for spontaneous adsorption of the single chain to occur, the enthalpy term in the Gibbs free energy of the system must be negative (i.e., adsorption must be an exothermic reaction). In other words, the interaction parameter $\chi_s$ with the surface must be larger than the interaction parameter $\chi$ between the polymer segment and the solvent. Due to the stronger attractive interaction, the segment must displace the solvent molecules and adsorb to the wall.

It is important to understand the significant differences in the adsorption behavior of small molecules and polymers. Whether small molecules or polymers, adsorption behavior is determined by the balance between the loss of entropy due to adsorption and the adsorption energy. However, for small molecules with the mole fraction $x$, the adsorption energy is approximately $kT\ln(x)$. If the adsorption energy is approximately $kT$, the adsorption occurs when $x > \frac{1}{e}$. In contrast, for polymers, it is sufficient for only a few segments out of a total of $n$ segments to adsorb. If $fn$ segments are involved in adsorption on a time average, the adsorption energy is $fnkT$, and adsorption occurs on the order of $x > \left(\frac{1}{e}\right)^{fn}$. $f$ is the fraction of adsorbed segments among all polymer segments. For typical polymers, $n$ is approximately 1,000. It means that the adsorption is supposed to occur at extremely low concentrations [32].

Regarding the theory construction of this loop-train-tail model, various theories have been proposed so far based on the Flory-Huggins theory [33–37]. Here, we will introduce one of the theories proposed by de Gennes using the scaling law [37].

The interfacial tension $\Gamma$ can be divided into two contributions as shown below:

$$\Gamma = \Gamma_d(\phi_s) + I(\phi_s, \phi_b) \tag{1.49}$$

where $\phi_s$ and $\phi_b$ are the volume fraction of polymer directly contacted with the wall and the volume fraction of the bulk, respectively, and $\Gamma_d(\phi_s)$ is the short-range interaction in the first layer of the adsorption layer, and $I(\phi_s, \phi_b)$ is the long-range interaction. $\phi_s$ is the extrapolated value of $\phi(z)$ at $z = 0$, and is associated with the value $\phi(a)$ as

$$\phi(a) = \frac{l}{2}\phi_s \tag{1.50}$$

where $\phi(a)$ is the value of $\phi(z)$ at $z = a$ in a lattice model with a lattice size of $a$, and $l$ is the train length.

Expanding $\Gamma_d(\phi_s)$ in $\phi_s$ and taking the first-order terms yields

$$\Gamma_d(\phi_s) = \Gamma_0 + \Gamma_1\phi_s \tag{1.51}$$

The terms above ${\phi_s}^2$ are related to the interaction between segments within the first layer and can be ignored under the condition of $\phi_s \ll 1$ which we consider here. This condition is easily realized for repulsive walls $\Gamma_1 > 0$ and also for attractive walls $\Gamma_1 < 0$ with the weak coupling limit as

$$|\Gamma_1| < kTa^{-2} \tag{1.52}$$

Furthermore, the fact that strong adsorption is realized even under the situation where the interfacial energy per unit volume is smaller than thermal energy is one of the characteristics of polymers. In other words, if $fn$ segments are adsorbed out of all segments, the adsorption energy is expressed as

$$fn|\Gamma_1|a^2 > kT \tag{1.53}$$

Before considering many terms of $\phi(z)$, let us consider a single polymer chain in a good solvent which is about to be adsorbed on an attractive wall. The chain is slightly attached to the wall, and the loop part extends to an average distance $D$ from the wall. In this case, the free energy per chain $F$ is

$$F \cong kT\left(\frac{R_F}{D}\right)^{\frac{5}{3}} - fn|\Gamma_1|a^2 \tag{1.54}$$

where $R_F$ is the Flory diameter and is defined as $R_F \cong n^{\frac{3}{5}}a$.

Since the polymer chain is spread over a thickness $D$, $f$ can be scaled as in the formula (1.55).

$$f \cong \frac{a}{D} \tag{1.55}$$

Substituting the formula (1.55) into (1.54) and minimizing the resulting (1.54) with respect to $D$, we get

$$f \cong \frac{a}{D} \cong \left(\frac{|\Gamma_1|a^2}{kT}\right)^{\frac{3}{2}} \tag{1.56}$$

$$\text{That is, } D \cong a^{-2}\left(\frac{|\Gamma_1|a^2}{kT}\right)^{-\frac{3}{2}} \tag{1.57}$$

Now let us consider a semi-dilute solution. According to the well-known scaling law, the correlation function $\xi_b$ becomes more significant than the Flory radius $R_F$ at the volume fraction $\phi_b$ greater than the overlap threshold volume fraction $\phi^* \cong n^{-\frac{4}{5}}$. Here, $\xi_b$ is the mesh size of entangled polymer chains, which is $\xi_b < R_F$. Under the two conditions that $\xi_b$ is independent of $n$ under $\phi_b < \phi^*$ and $\xi_b \sim R_F$ when $\phi_b \sim \phi^*$,

$$\xi_b(\phi_b) \cong a\phi_b^{-\frac{3}{4}} = ag^{\frac{3}{5}} \tag{1.58}$$

Therefore, $g \cong \phi_b^{-\frac{5}{4}}$

where $g$ is the number of segments per blob.

In this case, the size of the chain is

$$R^2(\phi_b) \cong \frac{n}{g}\xi_b{}^2 \cong na^2\phi_b^{-\frac{1}{4}} \tag{1.59}$$

In the case of $z > \xi_b$, the profile of $\phi(z)$ get closer to the bulk value, thus

$$\frac{\phi(z) - \phi_b}{\phi_b} \sim \exp\left(-\frac{z}{\xi_b}\right) \tag{1.60}$$

The profile $\phi(z)$ in $D < z < \xi_b$ is more interesting. In this region, $\phi(z)$ is independent from $\phi_b$. The formula (1.58) has now $z$ dependence due to the presence of the wall. Therefore, it is necessary to replace $\phi_b$ by $\phi(z)$ and set it as $\xi(\phi) \cong a\phi^{-\frac{3}{4}}$. However, in order to consider the scaling law with respect to $\xi$ in this region, the only physical parameter with the dimension of length is supposed to be $z$ itself, thus in the end, we have no choice but to set $\xi\left[\phi(z)\right] \cong z$. In other words, the mesh size has self-similarity that is scaled in the same way as $z$. From these discussions, we obtain $\phi(z) = \left(\frac{a}{z}\right)^{\frac{4}{3}}$. Considering the connectivity with the region of $z \sim a < D$,

$$\left|\frac{1}{\phi}\frac{d\phi}{dz}\right|_{z\to 0} = \frac{1}{D} \tag{1.61}$$

In the end, we can obtain the final form of $\phi(z)$

$$\phi(z) \sim \left(\frac{a}{z + \frac{3}{4}D}\right)^{\frac{4}{3}} \tag{1.62}$$

Based on this,

$$\phi_s = \phi(z = 0) \cong \left(\frac{a}{D}\right)^{\frac{4}{3}} \tag{1.63}$$

where $D$ in the formulas (1.62) and (1.63) is defined in the formula (1.57).

As for the thickness of the adsorption layer $t$,

$$t \sim \int_0^{R_F} z\phi(z)dz \sim R_F^{\frac{2}{3}} \sim n^{\frac{2}{5}} \tag{1.64}$$

It is found that the molecular weight dependence exponent of 2/5 (=0.4) is in surprising agreement with the exponent of 0.4 obtained experimentally by ellipsometry.

We will complete the introduction of the fundamentals of polymers. For readers unfamiliar with polymers, the contents in this chapter may be too advanced to be called "fundamentals." This is because we focus on the topics not described in other general textbooks on polymers. There are many polymer textbooks that cover more general basics of polymers. Thus, you should refer to such general polymer textbooks as well. In the next chapters, we will introduce the thermal expansion of polymers.

## References


1. Berry, G.C. and Fox, T.G. (1968). The viscosity of polymers and their concentrated solutions. *Adv. Polym. Sci.*, 5, 261–357.
2. Wu, S. (1989). Chain structure and entanglement. *J. Polym. Sci Part B Polym. Phys.*, 27, 723–741.
3. Levers, P.S. and Williams, J.G. (1985). Material and geometry effects on crack shape in double torsion testing. *J. Mater. Sci.*, 20, 77–84.
4. The Japan Polymer Society (2020). *Basic Polymer Science, 2nd ed.*, Tokyo Chemical Co., Ltd., Tokyo.
5. Flory, P.J. (1953). *Principles of Polymer Chemistry*, Cornell University Press, New York.
6. Hasegawa, M. and Nishi, T. (2009). *Basic Polymer Science*, Shoko-do Co. Ltd., Tokyo.
7. Inoue, S. and Miyata, S. (1993). *Chemistry of Polymer Materials, 2nd ed.*, Maruzen, Tokyo.
8. Matsushita, Y., Kanaya, T., Watanabe, H., Shimomura, T., Sato, T., Ito, K., Tanaka, K. and Inoue, T. (2013). *Structures and Physical Properties of Polymers*, Kodansha Scientific, Tokyo.
9. Bovey, F.A. and Winslow, F.H., Ed. (1981). *Macromolecules: An Introduction to Polymer Science*, Academic Press, London.
10. Stroble, G.R. (1996). *The Physics of Polymers*, Springer Verlag, Berlin.
11. Hosemann, R. (1962). Crystallinity in high polymers, especially fibres. *Polymer*, 3, 349–392.
12. Natta, G., Corradini, P. and Gains, P. (1960). Crystal structure of isotactic polypropylene. *Makromol. Chem.*, 39, 238–242.
13. Bunn, C.W. and Garner, E.V. (1947). The crystal structures of two polyamides ('nylons'). *Proc. R. Soc. Lond. A*, 189, 39–70.

**14** SABIC. (n.d.). https://www.sabic.com/en/products/specialties/noryl-resins/noryl-resin.

**15** Ougizawa, T. (2007). Interface of polymers. *J. Jpn. Colour Mater.*, 80, 390–396.

**16** Cahn, J.W. and Hilliard, J.E. (1958). Free energy of a nonuniform system. I. Interfacial free energy. *J. Chem. Phys.*, 28, 258–267.

**17** Nose, T. (1976). Theory of liquid—liquid interface of polymer systems. *Polym. J.*, 8, 96–113.

**18** Nose, T. (1991). Theoretical consideration on liquid-liquid interface in polymer systems. *J. Jpn. Soc. Colour Mater.*, 64, 729–738.

**19** Helfand, E. and Tagami, Y. (1972). Theory of the interface between immiscible polymers II. *J. Chem. Phys.*, 56, 3592–3601.

**20** Helfand, E. (1975). Theory of inhomogeneous polymers: Fundamentals if the Gaussian random-walk model. *J. Chem. Phys.*, 62, 999–1005.

**21** Wu, S. (1970). Surface and interfacial tensions of polymer melts. II. Poly(methyl methacrylate), poly(n-butyl methacrylate), and polystyrene. *J. Phys. Chem.*, 74, 632–638.

**22** Wu, S. (1988). A generalized criterion for rubber toughening: The critical matrix ligament thickness. *J. Appl. Polym. Sci.*, 35, 549–561.

**23** Roe, R.J. and Zin, W.C. (1980). Determination of the polymer-polymer interaction parameter for the polystyrene-polybutadiene pair. *Macromolecules*, 13, 1221–1228.

**24** Nishi, T. and Kwei, T.K. (1975). Cloud point curves for poly(vinyl methyl ether) and monodisperse polystyrene mixtures. *Polymer*, 16, 285–290.

**25** Ougizawa, T., Inoue, T. and Kammer, H.W. (1985). UCST and LCST behavior in polymer blends. *Macromolecules*, 18, 2089–2092.

**26** Akiyama, S., Inoue, T. and Nishi, T. (1981). *Polymer Blends*, Tokyo Kagaku Dojin, Tokyo.

**27** Paul, D.R. and Newman, S., Ed. (1978). *Polymer Blends Volume 1*, Academic Press, New York.

**28** Flory, P.J., Orwoll, R.A. and Vrij, A. (1964). Statistical thermodynamics of chain molecule liquids. I. An equation of state for normal paraffin hydrocarbons. *J. Am. Chem. Soc.*, 86, 3507–3514.

**29** (1). Dee, G.T. and Walsh, D.J. (1988). Equations of state for polymer liquids. *Macromolecules*, 2, 811–815. (2). Dee, G.T. and Walsh, D.J. (1988). A modified cell model equation of state polymer liquids. *Macromolecules*, 2, 815–817.

**30** Sanchez, I.C. and Lacombe, R.H. (1976). An elementary molecular theory of classical fluids. Pure fluids. *J. Phys. Chem.*, 80, 2352–2362.

**31** Fleer, G.J. and Lyklema, J. (1983). *Adsorption from Solution at the Solid/Liquid Interface* (Ed. G.D. Parfit and C.H. Rochester), 153, Academic Press, New York.

**32** Silberberg, A. (1971). The behavior of macromolecules at phase boundaries. *Pure Appl. Chem.*, 26, 583–591.

**33** Hoeve, C.A.J. (1965). Density distribution of polymer segments in the vicinity of an adsorbing interface. *J. Chem. Phys.*, 43, 3007–3008.

**34** Hoeve, C.A.J. (1966). Adsorption isotherm for polymer chains adsorbed from solvents. *J. Chem. Phys.*, 44, 1505–1509.

**35** Silberberg, A. (1967). Adsorption of flexible macromolecules. III. Generalized treatment of the isolated macromolecule; the effect of self-exclusion. *J. Chem. Phys.*, 46, 1105–1114.

**36** Silberberg, A. (1968). Adsorption of flexible macromolecules. IV. Effect of solvent-solute interactions, solute concentration, and molecular weight. *J. Chem. Phys.*, 48, 2835–2851.

**37** de Gennes, P.G. (1981). Polymer solutions near an interface. Adsorption and depletion layers. *Macromolecules*, 14, 1637–1644.